

Frequency-dependent demagnetisation rate of a shielded HTS tape stack

Lukasz Tomkow^{1,a}, Vicente Climente-Alarcon¹, Nikolay Mineev^{1,2}, Anis Smara¹, Bartek A. Glowacki^{1,3,4}

¹Applied Superconductivity and Cryoscience Group, Department of Materials Science and Metallurgy, University of Cambridge, Cambridge, CB3 0FS, United Kingdom

²Bruker BioSpin AG, Industriestrasse 26, Faellanden 8117, Switzerland

³Institute of Power Engineering, Warsaw 02-981, Poland

⁴Epoch Wires Ltd. Cambridge CB22 6SA, UK

E-mail: ^al1tt27@cam.ac.uk

Abstract. This work presents results of investigation of crossed-field demagnetization in 2G high temperature superconducting stacks at temperatures in the range of 77 - 20 K and in a variable frequency, corresponding to the particular rotor application.

We propose a method to reduce the demagnetization rate for a given stack configuration necessary for the superconducting rotor operating at a cryogenic temperature. This technique involves 3-D wrapping the stack of tapes with perpendicular layers of similar superconducting properties.

Previous 'proof of concept' studies documented some improvements in flux demagnetisation reduction for basic configuration. In the present study a more advanced approach based on magnetic flux shielding is adopted. The presented results provide an important contribution to development for design solutions that aim to increase the operational time before remagnetisation of the stacks would be required.

1. Introduction

Superconducting tapes consolidated to form stacks can be used as trapped-field magnets [1], with very high achievable magnetic induction of 17.7 T [2]. Such magnets can be used in place of permanent magnets in a superconducting motor [3]. However, some obstacles exist. An external cross-field present in a motor greatly accelerates demagnetisation [4], leading to the decrease of the power of the machine. The magnetisation and demagnetisation of the stacks for a superconducting motor was investigated experimentally and numerically [5, 6]. Additionally it causes heat generation, exacerbating the power decay [7].

Remagnetisation techniques and shielding can be applied to combat this problem [8]. Superconductors are well known for their shielding properties. However, the usage of the solid bulks would limit or prevent the magnetisation [9, 10, 11]. A shield made of electrically connected superconducting tapes would behave similarly [12]. The application of a shield surrounding the stack and covered with mu-metal was proposed [13]. Such shielding was observed to decrease a direct current decay in an YBCO coil subjected to external magnetic field [14].

The goal of this work is to investigate the effect of the application of different shielding methods. Two methods of shielding are considered. The first is the application of a contiguous shield



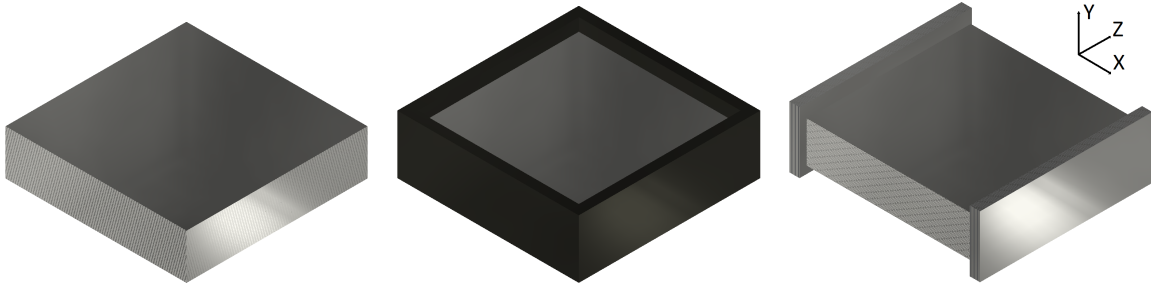


Figure 1. Variants of shielding; left to right - unshielded stack, closed shield, open shield

surrounding the stack and allowing the current to flow around it. The realisation of such shield would require either a bulk superconductor or a closed loop of tape [10, 12]. In this paper this type of shield is referred to as *closed*. The second method is the application of separate sets of tapes perpendicular to the stack either made of a single long piece of the tape surrounding the stack or a shield similar to the one described at [15], made of short overlapping pieces of tape. Such shield is called *open* in this paper. Examples of shielding variants analysed in this paper are shown in figure 1. The proposed shields can be used in different configurations and can be made to cover the stacks with complex shapes, such as the ones present in the superconducting motor [16].

2. Methods

To analyse the shielding behaviour of the superconductors protecting the stack a numerical model is created in Comsol Multiphysics using H-formulation [17]. It is assumed that the stack is long and its central cross-section along axis z is modelled, as shown in figures 1, 2 and 3. The tapes in a stack are stacked along y -axis, while an open shield is stacked along x -axis. Therefore a symmetry can be utilised and a 2D model can be applied. In this case the basic equation of H-formulation is equation 1 [18]. To simplify the calculations the stack and shields are homogenised and modelled as a single bulk.

$$\frac{\partial H_x}{\partial t} + \frac{\partial H_y}{\partial t} + \frac{\partial}{\partial x} (E_z(J_z)) - \frac{\partial}{\partial y} (E_z(J_z)) = 0 \quad (1)$$

H is here a local strength of magnetic field, t is time, E is electric field, J is current density. z -component of electric field E_z (out of model plane) is calculated using power law (equation 2).

$$E_z = \begin{cases} E_0 \left(\frac{|J_z| - J_c}{J_c} \right)^n \frac{J_z}{|J_z|} & \text{when } |J_z| \geq J_c \\ 0 & \text{when } |J_z| < J_c \end{cases} \quad (2)$$

J_c is here critical current. n is assumed as 31, E_0 as $100 \mu\text{V} \cdot \text{m}^{-1}$ [19, 20]. J_z is found using equation 3.

$$J_z = \frac{\partial H_x}{\partial y} - \frac{\partial H_y}{\partial x} \quad (3)$$

Critical current density in the modelled tapes is anisotropic. To account for this and the orientation of the tapes in the stack the method described at [20] is used, with material parameters (J_{c0} and B_0) fitted with data from [21]. J_c is calculated with equation 4.

$$J_c = J_{c0} \left[1 + \epsilon \frac{B^\alpha}{B_0} \right]^{-\beta} \quad (4)$$

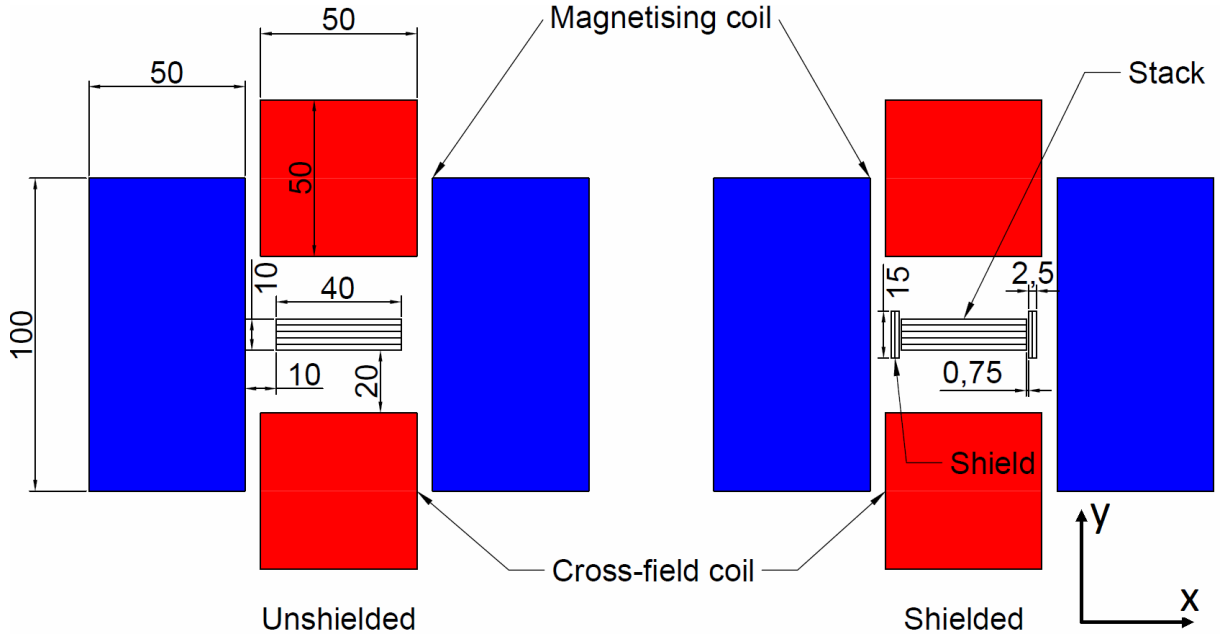


Figure 2. Geometry of the model

α , β and γ are based on the ones reported for SCS6050 tape, their values are 1, 0.67 and 2.77 respectively. B is the local strength of magnetic induction. ϵ depends on the direction of magnetic field and is calculated with equation 5.

$$\epsilon = \sqrt{\gamma^{-2} \cdot \left(\frac{B_x}{B}\right)^2 + \left(\frac{B_y}{B}\right)^2} \quad (5)$$

This equation is valid for the stack region, where the tapes are placed parallel to x axis. In the case of magnetic shields components x and y replace each other. The value of critical current is adjusted to reflect the actual share of superconducting material in a superconducting tape. The superconducting material is modelled as homogeneous to simplify the calculations.

In the non-superconducting regions E is calculated using equation 6, where ρ is the resistivity of a material.

$$E = \rho \cdot J_z \quad (6)$$

Geometry of the model is shown in figure 2. The stack is placed horizontally, with surface of the tapes parallel to x -axis. Two coils are positioned around the stack. Vertical one generates magnetising field along y -axis, horizontal - demagnetising cross-field along x -axis. Both are modelled as external current densities flowing in z direction. The remaining region is assumed to be air with relative magnetic permeability of 1.

Dense structured mesh is applied in the region of the stack. In shielded configuration the same type of mesh is used to model the shielding tapes. Geometry of the shield is not changed when different variants of shield winding are analysed. The thickness of the shield is assumed as 250 μm and critical current density is adjusted so the total critical current of the shield matches that of the used tapes.

Magnetising pulse is the same for every configuration. It is a symmetric trapezoidal pulse, lasting 0.3 s with 0.1 s plateau. The maximum strength of the magnetic induction in the centre of the considered region is 6 T. The magnetisation with such pulse is not full, reflecting the actual conditions in the motor. Demagnetising field has sinusoidal form and the strength of 1.95 T in

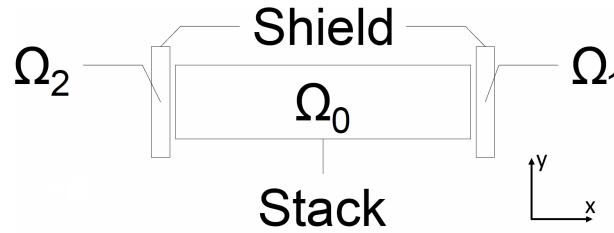


Figure 3. Regions of the model

the centre of considered region. Its frequency depends on the considered case and is varied from 0.5 to 500 Hz. The calculations are performed over the span of 500 cycles for each frequency. The behaviour of the superconductor in different cases is regulated by changing the constraints on current density imposed in the superconducting region. The names of the regions are presented in figure 3. Initially, an unshielded stack is modelled and the constraint described with equation 7 is used in region Ω_0 representing the stack. The same constraint is in effect in the stack region in both following cases.

$$\iint_{\Omega_0} J_z dx dy = 0 \quad (7)$$

In the case of closed shield the total current in the cross-section shield is set to 0 with the constraint described with equation 8, with Ω_1 and Ω_2 denoting regions of each tape.

$$\iint_{\Omega_1} J_z dx dy + \iint_{\Omega_2} J_z dx dy = 0 \quad (8)$$

In the case of an open shield two independent sets of tapes are placed on two sides of the stack, perpendicularly to the expected direction of a demagnetising field as proposed at [8]. In this case the constraint described with equation 7 is imposed separately on shield regions Ω_1 and Ω_2 , according to equation 9. With such constraint the total current in each shield is 0 and the formation of loops is forced.

$$\iint_{\Omega_1} J_z dx dy = \iint_{\Omega_2} J_z dx dy = 0 \quad (9)$$

The goal of shielding is to increase the magnetic flux trapped in the stack and decrease of the demagnetisation rate. For the purpose of comparison the trapped flux is calculated by the integration of y component of the magnetic field on the upper surface of the stack. Demagnetisation rate is analysed as time constant. To define the final expected value of magnetic flux generated by the trapped-field magnet Φ_0 and time constant τ the results are fitted to function 10. Φ is instantaneous value of magnetic flux, C is a constant marking the total reduction of magnetic field and t is time.

$$\Phi(t) = \Phi_0 + Ce^{-\frac{t}{\tau}} \quad (10)$$

3. Results and Discussion

The application of different methods of shielding affects the distribution of current density and magnetic induction. Figure 4 shows magnetic field and current density in direction z after magnetisation with the view zoomed on stack. Figure 4a shows the magnetic field trapped by

the unshielded stack. Two loops can be seen to form inside the stack in each case. The external loop is responsible for the generation of the magnetic field acting in the desired direction (same as the magnetising field).

In a closed shield the electric current after magnetisation flows in around the stack (figure 4b), contributing to the trapped field and increasing its strength. It can be seen that the magnetising loop inside the stack is smaller in this case and the magnetisation of the stack itself is actually weaker. In the case of an open shield the increase of trapped field is also observed, though the effect is weaker and comes mostly from trapping some of the stray field (figure 4c).

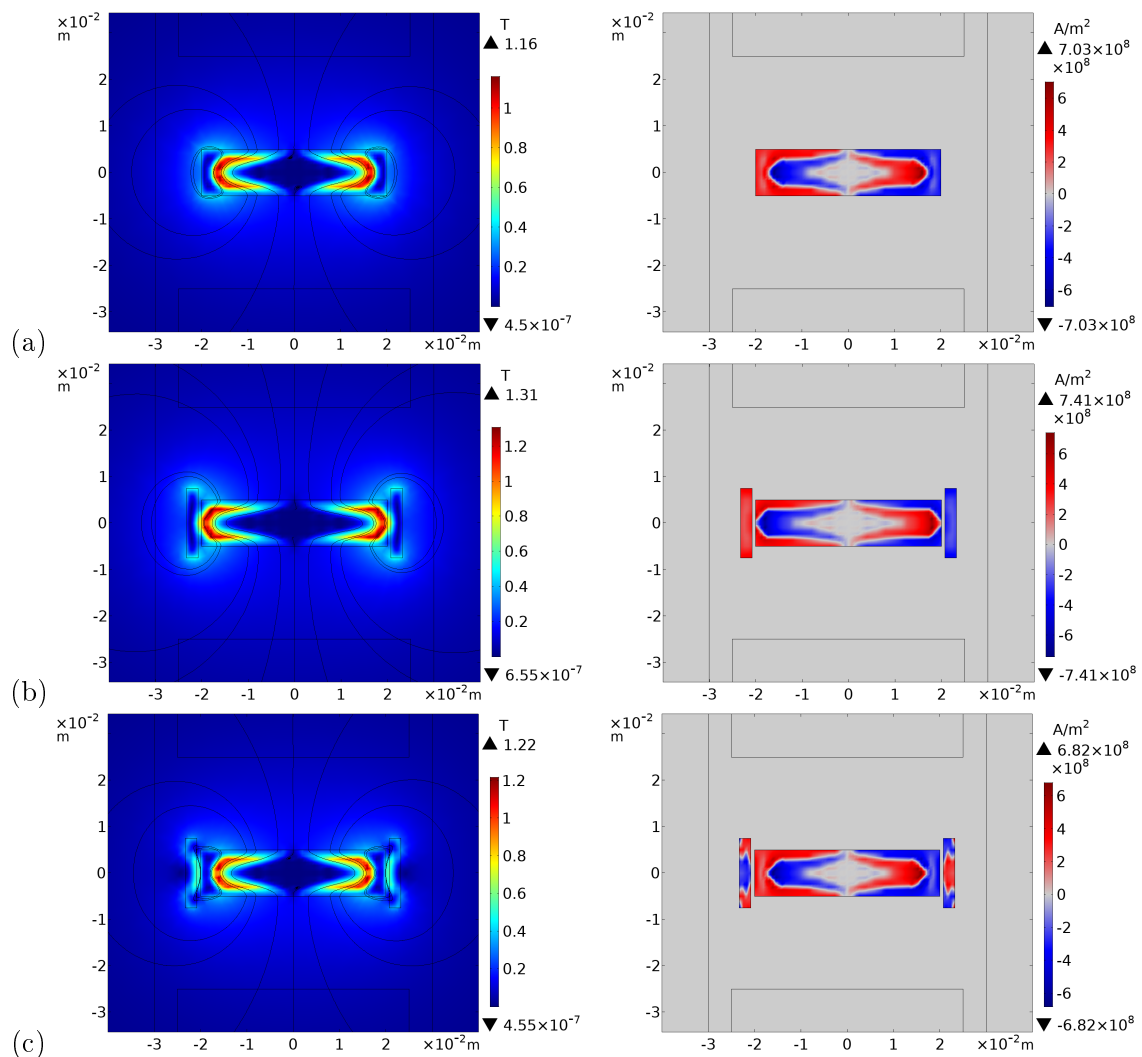


Figure 4. Magnetic induction (left) and current density (right) after magnetisation for (a) unshielded stack, (b) stack shielded with a closed shield, (c) stack shielded with an open shield

Magnetic induction and current distributions after demagnetisation for unshielded and different shielding configurations after 500 cycles at 50 Hz are shown in figure 5. In unshielded configuration the majority of magnetising current is washed out. The remaining loops from cross-field generate a negligible distortion of the field. The maximum current density is significantly lower than in remaining cases.

Some of the demagnetising field is preserved in the shielded stacks after demagnetisation and the patterns are distorted. In both cases additional parts of magnetising loops of electric current

are preserved, especially close to the end of the stack. Closed shield again contributes to the trapped field and magnetising loop clearly takes smaller part of the width of the stack than it is observed in other cases. A complex pattern of currents is visible in the case with open shield and some stray field is trapped by the shield.

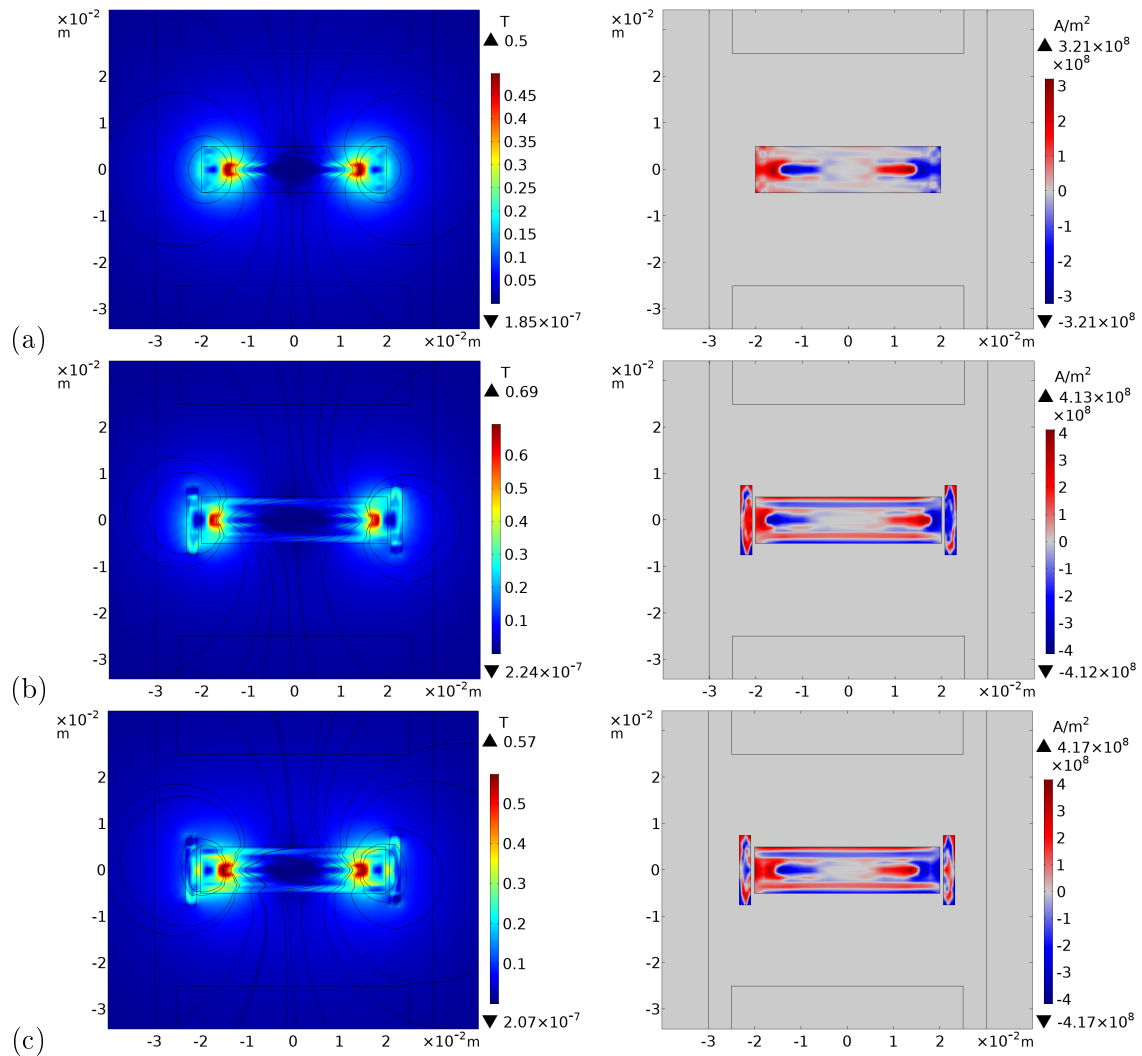


Figure 5. Magnetic induction (left) and current density (right) after 500 cycles of demagnetisation at 50 Hz for (a) unshielded stack, (b) stack shielded with a closed shield, (c) stack shielded with an open shield

Figures 6 and 7 show the size of trapped magnetic flux as function of number of cycles and time for different frequencies of demagnetising field and shielding configuration. Trapped magnetic field is larger with the shielded stack for every configuration and frequency. The higher initial value of trapped flux in the configuration with the connected shield is clearly visible in figure 6. However, the final magnetic field after demagnetisation is similar for both types of shielding. Final magnetic flux significantly increases with frequency, as seen also in figure 8. Low frequency demagnetising field is observed to quickly remove magnetisation in the case of unshielded stack. The final flux increases roughly logarithmically with frequency for both unshielded and shielded stacks, especially at higher frequencies. Protection by shields allows some additional magnetisation to remain. While strength of protected field after demagnetisation is similar with

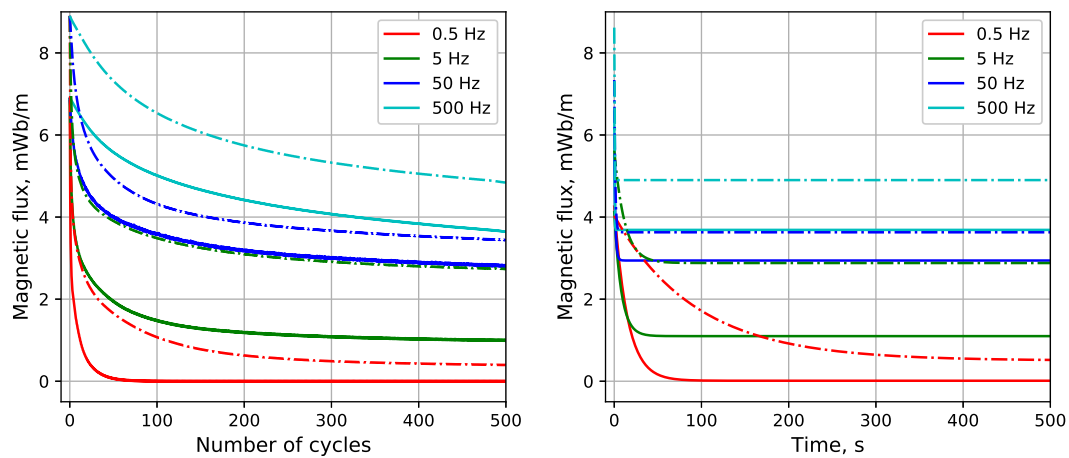


Figure 6. Magnetic flux against number of cycles (left) and time (right) for the stack shielded with a closed shield. Solid lines - unshielded, dash-dotted lines - shielded; the values on the plot versus time are based on fit for shielded and unshielded stack

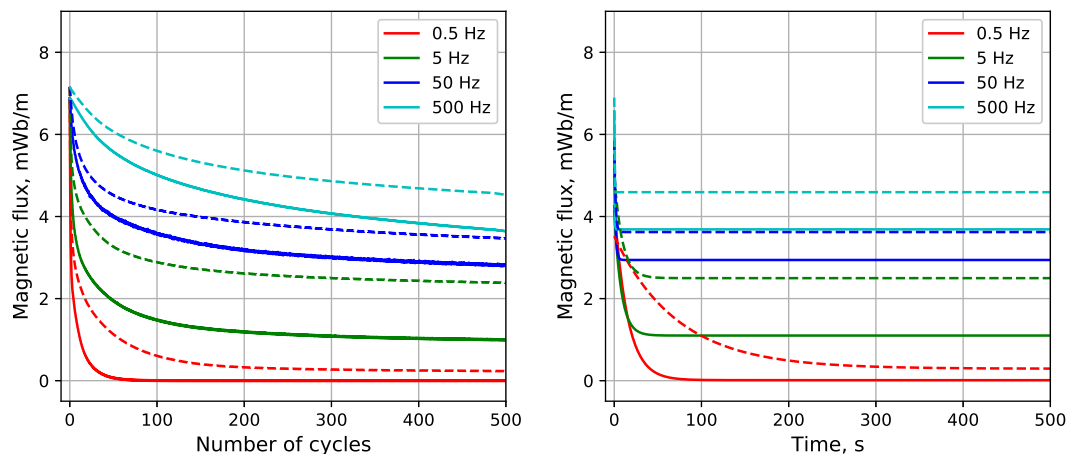


Figure 7. Magnetic flux vs number of cycles (left) and time (right) for the stack shielded with an open shield. Solid lines - unshielded, dashed lines - shielded; the values on the plot versus time are based on fit for shielded and unshielded stack

both shielding methods, it is slightly larger for closed shield.

Demagnetisation rate increases with frequency of demagnetising field, visible as the decrease of time constant in figure 8. Application of shields helps to decrease demagnetisation rate at low frequencies (up to approximately 5 Hz). Both open and closed shields have similar efficiency in this regard with closed shield again being slightly better. In the frequency range relevant to the operation of a superconducting motor (50-200 Hz) the shielding effect on demagnetisation rate is negligible.

Obtained results show that both types of shielding have similar efficiency in protecting the stack from demagnetisation. However, the nature of the protection is different. A closed shield is magnetised and holds some of trapped flux by itself. The stack itself is less magnetised. An open shield protects the magnetisation in the stack and does not carry any significant magnetising current. An open shield is easier and cheaper to realise than closed shield. It can be done with

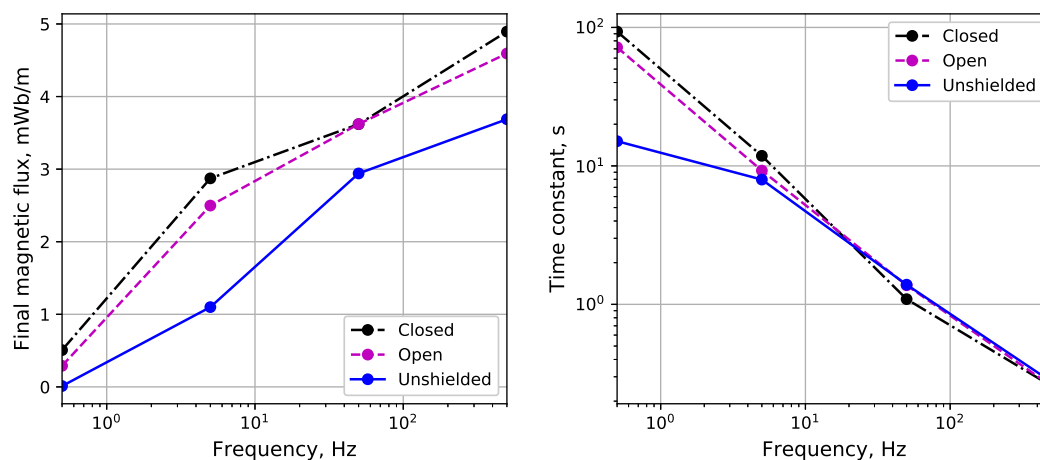


Figure 8. Left - final magnetic field vs frequency of demagnetising field, right - time constant vs frequency of demagnetising field

short pieces of tapes. Since closed loops of current around the protected stack are not formed it does not require superconducting joints or the application of bulks.

The analysis of the shielded stack with a 2D numerical model has some limitations. Possible complex effects on corners may appear decreasing the efficiency of the shield in this region. The investigation of these effects would require the application of 3D model. Initial experimental results reported at [8] are promising and further research will be performed. The improvement of resistance of the trapped-magnets to demagnetisation is crucial for any application in rotating machines.

4. Conclusions

Solving the problem of demagnetisation is crucial for the applicability of superconducting trapped field magnets. Efficient shielding can increase the power that can be generated with a motor by increasing trapped magnetic field and prevent some of demagnetisation. Two types of magnetic shields, open and closed, are analysed in the context of protection of a superconducting stack serving as a trapped field magnet. The shields differ in the way they protect the stack, but perform similarly.

Both types of shielding are observed to decrease demagnetisation rate at low frequencies and increase a final trapped magnetic flux. Closed shields increase trapped flux by carrying an additional magnetising current, while open shields decrease cross-field affecting the stack. Open shields seem to be better solution due to the simplicity of manufacturing and low price. The final magnetic flux depends on the logarithm of the frequency of demagnetising field for both shielded and unshielded stacks.

Further experimental and numerical analysis will be performed. A 3D-model will be created to investigate the effects at the ends of the shield. Experimental measurements of the behaviour of the shielded stacks in an actual motor are planned.

Acknowledgements

This research is financially supported partially by the European Union's Horizon 2020 research innovation programme under grant agreement No. 7231119 (ASuMED "Advanced Superconducting Motor Experimental Demonstrator") and also by EPSRC grant No. EP/P000738/1 entitled "Development of superconducting composite permanent magnets for

synchronous motors: an enabling technology for future electric aircraft".

References

- [1] Baskys A, Patel A, Hopkins S C, Kalitka V, Molodyk A and Glowacki B A 2015 *IEEE Transactions on Applied Superconductivity* **25** 1–4 ISSN 1051-8223
- [2] Patel A, Baskys A, Mitchell-Williams T, McCaul A, Coniglio W, Hänisch J, Lao M and Glowacki B A 2018 *Superconductor Science and Technology* **31** 09LT01 URL <https://doi.org/10.1088/1361-6668/aad34c>
- [3] Climente-Alarcon V, Patel A, Baskys A and Glowacki B A 2019 *IOP Conference Series: Materials Science and Engineering* **502** 012182 URL <https://doi.org/10.1088/1757-899x/502/1/012182>
- [4] Park M, Choi M, Hahn S, Cha G and Lee J 2004 *IEEE Transactions on Applied Superconductivity* **14** 1106–1109 ISSN 1051-8223
- [5] Tomkow L, Smara A, Climente-Alarcon V and Glowacki B A 2019 *Journal of Superconductivity and Novel Magnetism* ISSN 1557-1947 URL <https://doi.org/10.1007/s10948-019-05375-3>
- [6] Smara A, Mineev N, Climente-Alarcon V, Patel A, Baskys A, Glowacki B A and Reis T 2019 *Superconductor Science and Technology* **32** 085009 URL <https://doi.org/10.1088/1361-6668/32/8/085009>
- [7] Climente-Alarcon V, Smara A, Patel A, Glowacki B A, Baskys A and Reis T 2019 Field cooling magnetization and losses of an improved architecture of trapped-field superconducting rotor for aircraft applications *AIAA Propulsion and Energy Forum and Exposition, Indianapolis, Indiana* p 3189332
- [8] Baskys A, Patel A and Glowacki B A 2018 *Superconductor Science and Technology* **31** 065011 URL <https://doi.org/10.1088/1361-6668/aabf32>
- [9] Hogan K, Fagnard J F, Wéra L, Vanderheyden B and Vanderbemden P 2015 *Superconductor Science and Technology* **28** 035011 URL <https://doi.org/10.1088/1361-6668/28/3/035011>
- [10] Tomkow L, Ciszek M and Chorowski M 2015 *Journal of Applied Physics* **117** 043901
- [11] Fagnard J F, Vanderheyden B, Pardo E and Vanderbemden P 2019 *Superconductor Science and Technology* **32** 074007 URL <https://doi.org/10.1088/1361-6668/32/7/074007>
- [12] Tomkow L, Ciszek M and Chorowski M 2016 *IEEE Transactions on Applied Superconductivity* **26** 1–4 ISSN 1051-8223
- [13] Baghdadi M, Ruiz H S, Fagnard J F, Zhang M, Wang W and Coombs T A 2015 *IEEE Transactions on Applied Superconductivity* **25** 1–4 ISSN 1051-8223
- [14] Geng J, Zhang H, Li C, Zhang X, Shen B and Coombs T A 2017 *Superconductor Science and Technology* **30** 035022 URL <https://doi.org/10.1088/1361-6668/30/3/035022>
- [15] Tomkow L, Kulikov E, Kozlowski K and Drobin V 2019 *Journal of Applied Physics* **126** 083903 URL <https://doi.org/10.1063/1.5112036>
- [16] Patel A, Climente-Alarcon V, Baskys A, Glowacki B A and Reis T 2018 Design considerations for fully superconducting synchronous motors aimed at future electric aircraft
- [17] Pecher R, McCulloch M, Chapman S and Prigozhin L 2003 *Proc. EUCAS 2003*
- [18] Zhang M, Kvitkovic J, Kim J H, Kim C H, Pamidi S V and Coombs T A 2012 *Applied Physics Letters* **101** 102602 URL <https://doi.org/10.1063/1.4749275>
- [19] Kvitkovic J, Patel S, Zhang M, Zhang Z, Peetz J, Marney A and Pamidi S 2018 *IEEE Transactions on Applied Superconductivity* **28** 1–5 ISSN 1051-8223
- [20] Zhang X, Zhong Z, Geng J, Shen B, Ma J, Li C, Zhang H, Dong Q and Coombs T A 2018 *Journal of Superconductivity and Novel Magnetism* URL <https://doi.org/10.1007/s10948-018-4678-8>
- [21] Zhang M, Kim J H, Pamidi S, Chudy M, Yuan W and Coombs T A 2012 *Journal of Applied Physics* **111** 083902 URL <https://doi.org/10.1063/1.3698317>